Catal Lett (2012) 142:698–713
DOI 10.1007/s10562-012-0818-0

Fischer–Tropsch Synthesis: Preconditioning Effects Upon Co-Containing Promoted and Unpromoted Catalysts

Donald C. Cronauer · Jeffrey W. Elam · A. Jeremy Kropf · Christopher L. Marshall · Pei Gao · Shelley Hopps · Gary Jacobs · Burtron H. Davis

Received: 6 January 2012 / Accepted: 23 March 2012 / Published online: 10 April 2012

Abstract In the preparation and evaluation of Fischer–Tropsch (FT) catalysts, active catalysts formed by both incipient wetness impregnation (IWI) and atomic layer deposition (ALD) of major components were demonstrated. ALD-deposited Co on a silica support was more effective than a similar catalyst deposited upon a support of ALD-deposited Al_2O_3 on silica. The addition of Co reduction promoters including Pt, Ir and Ru using either ALD or IWI has been shown to strongly affect the catalyst pre-conditioning step. CO conversion results were consistent with previously reported Temperature Programmed Reduction X-ray Absorption Near-edge Structure/Extended X-ray Absorption Fine Structure Spectroscopy (TPR-XANES/EXAFS) experiments observing the nature of chemical transformations occurring during the activation of cobalt-based FT catalysts in hydrogen. Specifically, there exists a 2-step reduction process involving Co_3O_4 to CoO and CoO to Co^0 transformations. The extent of catalyst preconditioning was strongly affected by the reduction temperature (with 400 °C preferred) and the loading of the promoter. This was demonstrated using a continuous-flow catalytic-bed unit with a 2:1 molar blend of H_2:CO, at temperatures ranging from about 260 to 300 °C, pressures averaging 1.3 MPa (190 psia), and gas space velocities about 24 NL/h-g.

D. C. Cronauer (✉) · J. W. Elam · A. J. Kropf · C. L. Marshall
Argonne National Laboratory, Argonne, IL 60439, USA
e-mail: dccronauer@anl.gov

P. Gao · S. Hopps · G. Jacobs · B. H. Davis
Center for Applied Energy Research, 2540 Research Park Drive, Lexington, KY 40511, USA

Keywords Fischer–Tropsch · Catalyst pretreatment · Promoters · Cobalt · Alumina · Incipient wetness impregnation · Atomic layer deposition · TPR · EXAFS · XANES

1 Introduction

Fischer–Tropsch (FT) chemistry involves the reaction of hydrogen with carbon monoxide to form long-chain hydrocarbons. Even though this process was invented in Germany in 1923, there has been a continuing development of catalysts, the most common of which are based upon iron, cobalt, and ruthenium. Due to the water gas shift catalytic activity of iron, its use in FT catalysis is often directed toward a gas stream generated from the gasification of coal (namely, lower H_2/CO ratios.) In the case of gas to liquid (GTL) production with higher H_2/CO ratios ($\sim$2:1), emphasis is often directed toward supported cobalt catalysts. Such processes typically use a supported cobalt catalyst (e.g. Co/Al_2O_3) under pressure (e.g., $\sim$20 bar) and mild temperatures (e.g., $\sim$220 °C) to produce a distribution of hydrocarbons—mainly straight chain paraffins—that can be upgraded to transportation fuels (e.g., diesel, jet fuel). Cobalt catalysts are relatively inactive intrinsically for the water–gas shift reaction. One drawback of cobalt is that it is more expensive than iron. Thus, catalyst activity must be maintained over long periods of time for the process to be economically viable.

The available literature on these catalysts is very extensive. For reference, a very comprehensive series of articles on the FT process has been edited by Schulz and Claeys [1] and Steynberg and Dry [2]; the kinetics literature was reviewed by Van der Laan and Beenackers [3]; see also Satterfield [4]. Davis has carried out an extensive

study of FT catalysis under DOE contracts; reference is made to the Final Technical Report [5] of Contract No. PC90056.

Two of the significant factors to be considered in the use of Co-containing catalysts are particle size and reducibility. Below a dispersion of 12 %, Iglesia [6] reported a linear trend between FT activity and cobalt surface area on a per gram of catalyst basis as measured by hydrogen chemisorption, indicating that the active sites for the catalysis are the surface cobalt metal particles. At higher dispersions, lower activity has been reported, although it is not clear if this is due to actual lower activity on small Co particles, or rather due to particle size dependent deactivation (e.g., reoxidation [7]). Bezemer et al. [8] explored the impact of particle size on turnover frequency in the range of 2.6–27 nm using 0.8–22 %Co supported on carbon-nanofibers. They found that the CO rate based on g of Co increases with Co size from 2.6 to 8.5 nm and then decreases between 8.5 and 16 nm. These data resulted in an increasing TOF with increasing Co particle size below 8 nm while above that size TOF remained stable. C_5+ selectivity displayed an increasing trend with increasing Co particle size up to 16 nm. Borg et al. [9] examined Co particle size effects in the range of 3-18 nm using 10–30 %Co/Al_2O_3 catalysts at 210 °C, 20 bar, and a H_2/CO ratio of 2.0. Employing a micro-fixed-bed reactor, the authors reported that the best Co particle size range for production of C_5+ was 7–8 nm.

Due to the strong interaction of alumina with cobalt oxides, alumina stabilizes very small cobalt oxide particles. The small particle size is important for producing a significant surface area of metallic cobalt following activation in H_2. However, the highly interacting small particles are difficult to reduce and thus, reduction promoters (e.g., Pt, Ru, and Re) are often employed—and often in combination—to facilitate reduction of the cobalt oxide crystallites to the metallic state.

Reduction of Co_3O_4 clusters takes place in two steps: (1) $Co_3O_4 + H_2 \rightarrow 3CoO + H_2O$ and (2) $3CoO + 3H_2 \rightarrow 3Co^0 + 3H_2O$ This two-step process has been recently demonstrated by a TPR-EXAFS/XANES investigation [10]. When the reduction promoter reduces below the temperature of step 1 (typically in the temperature range of 300–350 °C), as in the case of Pt or Ru both steps are typically shifted to lower temperatures [11–14]. However, in the case of Re [11, 12, 15, 16] which reduces at a comparable temperature to the first step, only the second reduction step (CoO to Co^0) has been observed to be impacted. Using a standard 10 h H_2 reduction treatment of 350 °C, Jacobs et al. [11] showed by hydrogen chemisorption/pulse reoxidation measurements that in all cases (Pt, Ru, and Re), gains in active site densities (i.e., number of cobalt atoms exposed at the surface) were directly due to the higher extents of reduction gained by promoter addition. The three promoters, Pt, Ru and Re, have all been observed to exhibit direct contact with Co at the atomic level by EXAFS spectroscopy [12, 17–20].

In this study we compare the performance of Co catalysts prepared using two different techniques, namely: (1) Incipient wetness impregnation (IWI) and (2) atomic layer deposition (ALD). IWI is a conventional catalyst preparation method in which the catalyst support is immersed in a solution of the desired metal salt, and then dried and calcined. ALD is a thin film growth technique utilizing alternating, self-limiting chemical reactions between gaseous precursors and a solid surface to deposit materials in an atomic layer-by-layer fashion [21]. Both uniform thin films as well as discrete nanoparticles can be formed by ALD. ALD has been shown to yield more highly dispersed surface species than IWI at comparable metal loadings in some cases [22]. Consequently, one objective of this study was to compare the relative performance of Co catalysts prepared using IWI and ALD to determine if there is any advantage for the ALD.

To provide an effective comparison between catalyst samples, a small charge (0.1 g) of catalyst was used. At a total gas feed rate of about 40 mL/min, the space velocity was about 24 standard liters per hour gram (SL/h g). For reference, the space velocity of the experiments of Jacobs et al. [11]. was about 2 SL/h g; therefore, our CO conversion rates should be lower than those typically reported for FT experiments.

2 Experimental

2.1 FT Reactor System

A continuous-flow catalytic-bed unit was used. The gaseous feed consisted of a 2:1 molar blend of H_2:CO. The feed passed through a preheater/reactor that consisted of a 0.4 cm-ID tube of 90 cm length. Gaseous flow was downward through the following zones:

1. An empty upper zone of about 46 cm filled with quartz wool zone to serve as a preheater,
2. A second zone of about 10 cm consisted of low-surface α-Al_2O_3 to ensure radial flow dispersion,
3. A third zone of about 3 cm consisted of supported catalyst that was mixed 6/0.1 with α-Al_2O_3,
4. A bottom zone of additional α-Al_2O_3 packing served to support the active catalyst mixture in the temperature controlled zone.

The α-Al_2O_3 packing above and below the reaction zone was 14 × 18 mesh, and 20 × 24 in the reaction zone.

The preheater and reactor had a total of six internal and two external thermocouples. The reactor temperature was controlled using a thermocouple near the center of the active catalyst bed. Two thermocouples located within the reaction zone typically averaged within 3 °C.

The experiments were carried out at temperatures ranging from about 220 to 300 °C, pressures averaging 1.3 MPa (190 psia), a gas feed rate of about 40 mL/min, and a catalyst charge of 0.1 g. The reactor effluent was cooled in air and then one of two parallel wet-ice-cooled traps so that periodic condensate samples could be recovered for weighing and sampling. The off-gas was pressure controlled, metered and sampled.

The gas composition was determined using an HP 6890 Series gas chromatograph (GC) that had been modified by LINC Quantum Analytics of Foster City, CA. It had three columns: (1) a molecular sieve column (7 ft × 1/16 in. 13 × 45/60) for light gas retention and separation, (2) a capillary column (50 m × 0.53 mm KCl modified Al_2O_3 PLOT) for hydrocarbon analysis by a flame ionization detector (FID), and (3) a packed column (7 ft × 1/16 in. Hayesep A 60/80) for CO_2 separation and analysis using a thermal conductivity detector (TCD). The calibration of the system was routinely carried out.

Emphasis was placed upon observing the extent of CO conversion. This was determined on a basis of C molar balance; namely 100 % minus the sum of the carbon-containing products. At a CO conversion level of 20 %, the typical C balance was >96 %, and the distribution was normalized to 100 %. The selectivity in forming CH_4 was about 4–5 %, that of C_2+ hydrocarbons was about 90 %, and that of CO_2 was about 3–5 %.

2.2 Catalyst Preparation

The IWI preparation procedures for the 25 % Co-catalyst samples have been previously described [10]. In addition, IWI was used to prepare samples of Pt and Ir promoted catalysts. Salts of $Pt(NH_3)_4(NO_3)_2$, or $Ir(acac)_3$ were dissolved in sufficient water to wet the above Co-containing catalyst. They were impregnated into the catalyst and subsequently dried and calcined in air at 200 °C for about 1 h after the total heat-up and drying stages of about 2 h.

Co-containing catalysts were also prepared using a viscous flow ALD reactor [23, 24] at 1.3 mbar (1 Torr) pressure using ultrahigh purity nitrogen carrier gas at a mass flow rate of 360 sccm and a temperature of 465 °C. Approximately 1 g of the silica gel support material was contained in a fixed-bed powder fixture. After allowing the powder to thermally equilibrate and outgas, the silica gel was cleaned using a 1.3 mbar (1 Torr), 400 sccm mixture of 10 % ozone in oxygen for 10 min. In selected cases, an Al_2O_3 ALD technique was used to deposit an additional catalytic support layer. The Al_2O_3 ALD used three ALD cycles comprised of alternating exposures to trimethyl aluminum and water vapors to deposit ~0.4 nm of Al_2O_3 [25–27]. Finally, the Co_3O_4 ALD coating was performed using 5–20 ALD cycles comprised of alternating exposures to bis(cyclopentadienyl)cobalt (II) and ozone. In addition to the silica gel powder, small portions of Si(100) wafers were coated concurrently with the ALD Co_3O_4 and subsequently analyzed using spectroscopic ellipsometry. These measurements determined that each ALD Co_3O_4 cycle deposits 0.23 nm of material. X-ray fluorescence measurements were performed on the silica gel powders to determine the cobalt loading. These measurements revealed that the Co_3O_4 ALD deposits ~1.7 wt % Co per ALD cycle on the S10040M powder.

Various promoted catalysts were prepared using ALD. Approximately 0.2 g of the above Co-based catalyst was contained in a fixed bed fixture. This catalyst was treated using alternating exposures to the noble metal precursor and oxygen to deposit ~1 nm nanoparticles. The noble metal precursors for Pt, Ir, and Ru were $Pt(MeCp)Me_3$, $Ir(acac)_3$, and 4-(dimethylpentadienyl)(ethylcyclopentadienyl) ruthenium (DER), respectively. Metal loadings of ~0.1 wt % were achieved by adjusting the deposition temperature in the range 100–300 °C as well as the number of ALD cycles performed. The specific details of the Pt deposition have been described in detail [21, 22]. Similar approaches were used to deposit the Ir and Ru.

Additional catalysts were prepared by applying thin films of aluminum oxide and cobalt oxide onto silica gel powder supports using ALD. The silica gel was Silicycle S10040M with a specific surface area of 100 m^2/g, a pore size of 30 nm and a particle size of 75–200 microns.

2.3 Catalyst Preconditioning

A two-step reduction process was observed [10] consisting of Co_3O_4 to CoO and CoO to Co^0 transformations over catalysts exhibiting both weak metal/support interactions (i.e., Co/SiO_2) and strong interactions (i.e., Co/Al_2O_3). Increased reduction temperatures were needed to effectively reduce Co-containing catalysts deposited on strongly interacting surfaces when compared with those of unsupported Co_3O_4 or weakly supported Co catalyst. The addition of noble metal promoter (i.e., Pt) strongly affected the reducibility and resulting cobalt crystallite size.

Cobalt-containing catalysts were preconditioned in flowing 100 % hydrogen at atmospheric pressure. The temperature was increased from room temperature to 350 °C in 1 h; the catalyst was then maintained at this temperature with 100 % hydrogen flow for about 6 h. Similar conditions were used for fresh catalyst conditioning at 400 °C. In selected cases, a catalyst that had been

preconditioned at 350 °C and used in FT experiments was further conditioned in flowing hydrogen at 400 °C at atmospheric pressure prior to subsequent FT experiments.

2.4 BET Measurements

BET measurements for the catalysts were conducted using a Micromeritics Tri-Star system. Prior to the measurement, samples were slowly ramped to 160 °C and evacuated for 24 h to approximately 50 mTorr (~0.2 mbar).

2.5 X-ray Diffraction

Powder diffractograms on calcined catalysts were recorded using a Philips X'Pert diffractometer. First, short times were used over a long range to assess crystalline phases present. The conditions were as follows: scan rate of 0.02°/step, scan time of 5 s/step over a 2θ range of 15–80°. Then, long times were used over a short range in order to quantify average Co_3O_4 domain sizes using line broadening analysis for the peak at $2\theta = 36.8°$ representing (311). The conditions employed for the latter were a scan rate of 0.01°/step and a scan time of 30 s/step over a 2θ range of 30–45°.

2.6 Hydrogen Chemisorption with Pulse Reoxidation

Hydrogen chemisorption measurements were performed using a Zeton Altamira AMI-200 unit, which utilizes a TCD. The sample weight was typically 0.220 g. The catalyst was activated at 400 °C for 5 h using a flow of pure hydrogen and then cooled under flowing hydrogen to 100 °C. The sample was then held at 100 °C under flowing argon to prevent physisorption of weakly bound species prior to increasing the temperature slowly to the activation temperature. At that temperature, the catalyst was held under flowing argon to desorb the remaining chemisorbed hydrogen so that the TCD signal returned to the baseline. The TPD spectrum was integrated and the number of moles of desorbed hydrogen determined by comparing to the areas of calibrated hydrogen pulses. Prior to experiments, the sample loop was calibrated with pulses of nitrogen in helium flow and compared against a calibration line produced from gas tight syringe injections of nitrogen under helium flow.

After TPD of hydrogen, the sample was reoxidized at the activation temperature by injecting pulses of pure oxygen in helium referenced to helium gas. After oxidation of the cobalt metal clusters, the number of moles of oxygen consumed was determined, and the percentage reduction calculated assuming that the Co^0 reoxidized to Co_3O_4. While the uncorrected dispersions (uc) are based on the assumption of complete reduction, the corrected dispersions (c), which are reported in this work, include the percentage of reduced cobalt as follows.

$$\%D_{uc} = (\#\text{ of } Co^0 \text{ atoms on surface} \times 100\,\%)/(\text{total } \#\ Co^0 \text{ atoms})$$

$$\%D_{c} = (\#\text{ of } Co^0 \text{ atoms on surface} \times 100\,\%)/[(\text{total } \#\ \text{Co atoms})(\text{fraction reduced})]$$

2.7 Catalyst Characterization by TPR-EXAFS/XANES with a Multi-Sample Holder

In situ H_2-TPR XAFS studies were performed at the Materials Research Collaborative Access Team (MR-CAT) beamline at the Advanced Photon Source, Argonne National Laboratory. A cryogenically cooled Si(1 1 1) monochromator selected the incident energy and a rhodium-coated mirror rejected higher order harmonics of the fundamental beam energy. The experiment setup was similar to that outlined by Jacoby [28]. A stainless steel multi-sample holder (4.0 mm i.d. channels) was used to monitor the in situ reduction of six samples during a single TPR run. Approximately 6 mg of each sample were loaded as a self-supporting wafer in each channel. The catalyst to diluent weight was approximately 0.1. Supported cobalt catalyst samples were diluted with sufficient SiO_2 to allow for the wafer to be self supporting. The holder was placed in the center of a quartz tube, equipped with gas and thermocouple ports and Kapton windows. The amount of sample used was optimized for the Co K edge, considering the absorption by Al and/or Si of the support. The quartz tube was placed in a clamshell furnace mounted on a positioning table. Each sample cell was positioned relative to the beam by finely adjusting the position of the table to an accuracy of 5 μm (for repeated scans). Once the sample positions were fine-tuned, the reactor was purged with helium for more than 5 min at 100 ml/min then the reactant gas (H_2/He, 4 %) was flowed through the samples (100 ml/min) and a temperature ramp of ~1.0 °C/min (starting from 250 °C after a more rapid startup) was initiated for the furnace. The Co K-edge spectra were recorded in transmission mode and a Co metallic foil spectrum was measured simultaneously with each sample spectrum for energy calibration. By measuring each sample, in turn, and repeating, this allowed 24 scans to be collected for each sample over an 8 h period. The sample's temperature change from the absorption edge through the end of the scan was then about 5.0 °C, while each sample was measured approximately every 30 °C starting from about 250 °C, following a more rapid startup. Data reduction of the EXAFS/XANES spectra was carried out using the WinXAS program [29]. The details of the XANES and EXAFS analyses are provided in the appendices of our previous article, and will not be repeated here, for the sake of brevity [10]. EXAFS data reduction and fitting were carried out using on the catalysts in their final state

following TPR and cooling using the WinXAS [29], Atoms [30], FEFF [31], and FEFFIT [32] programs. The k-range used for the fittings was 3–12 $Å^{-1}$. Fitting was confined to the first Co–Co metallic coordination shell by applying a Hanning window in the Fourier transform magnitude spectra, and carrying out the back-transform to isolate that shell.

3 Results and Discussion

3.1 BET Characterization

BET results for supports and, where possible, catalysts, are reported in Table 1. For the catalysts prepared by aqueous impregnation on γ-Al_2O_3, 25 % of Co is equivalent to about 33 % Co_3O_4 by weight. If alumina is the main contributor to the surface area, then if no pore blocking occurs, the surface area of the catalysts should be $0.67 \times 150\ m^2/g = 100\ m^2/g$. Most of the catalysts were within 5 m^2/g of this value. However, one catalyst, 0.1 %Pt (ALD) 25 %Co (IWI) Al_2O_3 was slightly lower, indicating some particles may have been large enough to cause some minor pore blocking. Similar findings were obtained in evaluating Co/SiO_2. With the ALD catalysts, the BET surface area was about 10 m^2/g lower when both Al_2O_3 and 25 %Co were deposited on SiO_2 relative to only deposition of 25 %Co.

3.2 Catalyst Characterization by XRD/Hydrogen Chemisorption-Pulse Reoxidation

XRD profiles are displayed in Figs. 1 and 2. Significant broadening of the (311) peak is observed whenever ALD was used to deposit cobalt as compared with the IWI method, regardless of support. Results of line broadening analysis for evaluating Co_3O_4 crystallite size in calcined catalysts, and projected Co^0 crystallite diameter following reduction, are summarized in Table 1, along with—where possible—results of hydrogen chemisorptions pulse reoxidation. The crystallite diameter from XRD was about half of that (5.6–5.9 nm relative to 10.1 nm) for the 25 %Co catalysts prepared on SiO_2 by ALD relative to 20 %Co/SiO_2 air calcined catalysts. The agglomeration of crystallites into large (52 nm) clusters was noted in chemisorption results for the 20 %Co/SiO_2 air calcined catalyst. Likewise, the crystallite diameter from XRD was a little more than half of that (6.7 nm relative to 10–11 nm) for the 25 %Co catalyst prepared on Al_2O_3 by ALD relative to the catalysts prepared by aqueous impregnation to 25 %Co levels. The sizes obtained by hydrogen chemisorption/pulse reoxidation were slightly smaller, but within experimental error, of those predicted from XRD. This may be due to the fact that XRD requires a certain degree of long range order. Unlike the air calcined 20 %Co/SiO_2 catalyst, the 25 %Co/Al_2O_3 catalysts maintained the small cluster size following activation.

3.3 Catalyst Characterization by TPR-EXAFS/XANES with a Multi-Sample Holder

TPR-XANES spectra are reported in Figs. 3 and 4. The extents of CoO reduction to Co^0 are plotted vs. temperature for all catalysts in Fig. 5. The extent of reduction vs. temperature overlays are plotted in Fig. 6. As demonstrated in our previous work [10], in each case, the catalyst begins with cobalt oxide particles as Co_3O_4. Unpromoted catalysts undergo the first reduction step from Co_3O_4 to CoO in the temperature range of ~350 °C, and Fig. 3c provides a reference for 25 %Co/Al_2O_3. The spectra for maximum CoO content were retrieved from each TPR trajectory and are plotted in Fig. 7. The maxima were slightly different, and may depend on support type [10]. The temperature at which maximum CoO content was achieved in the reference 25 %CoAl_2O_3 catalyst was measured to be 360.2 °C. Addition of a small amount of Pt (i.e., ~0.1 %) by IWI facilitated reduction of the first step considerably, with the temperature for maximum CoO content decreasing to a narrow range of 308–313 °C for the two Pt promoted 25 %CoAl_2O_3 catalysts. Using the ALD method, however, decreased the temperature even further, to 288 °C. The temperature for the catalyst having 0.1 % Pt (ALD) 25 % Co(ALD)/Al_2O_3(ALD) on SiO_2 was ~322.0 °C, slightly higher than the three 0.1 %Pt/25 %Co/Al_2O_3 catalysts. However, the corresponding temperature for the 0.1 %Pt(ALD) 25 %Co (ALD)/SiO_2 was in the same range as the 0.1 %Pt/25 %Co/Al_2O_3 catalysts, at 297 °C.

The more important reduction step is that of CoO to Co^0, since Co^0 is active for CO hydrogenation (e.g., Fischer–Tropsch synthesis). The temperature at which 50 % conversion from CoO to Co^0 was achieved in the reference 25 %CoAl_2O_3 catalyst was measured to be 455.9 °C. Adding a small amount of Pt (i.e., ~0.1 %) by IWI also facilitated reduction of the second step considerably, with the temperature for 50 % conversion of CoO to Co^0 decreasing to a narrow range of 390.5–399.7 °C for the two Pt promoted 25 %CoAl_2O_3 catalysts. Again, however, using the ALD method decreased the temperature even further, to 352.4 °C. The corresponding temperature for the catalyst having 0.1 % Pt (ALD) 25 % Co(ALD)/Al_2O_3(ALD) on SiO_2 was ~412.86 °C, slightly higher than the three 0.1 %Pt/25 %Co/Al_2O_3 catalysts. On the other, the corresponding temperature for the 0.1 %Pt(ALD) 25 %Co (ALD)/SiO_2 was even somewhat lower than the 0.1 %Pt/25 %Co/Al_2O_3 catalysts, at 342.8 °C.

The TPR-EXAFS results are reported in Figs. 3 and 4. In each case, there is initially a strong signal for Co–O

Table 1 Results of BET surface area, X-ray diffraction, and hydrogen chemisorption/pulse reoxidation

Catalyst	BET SA, m^2/g	Ave. pore vol., cm^3/g	Ave. pore rad., nm	Diam. Co_3O_4 from XRD, nm	Est. diam. Co^0 from XRD, nm	H_2 desorbed per g_{cat}, µmol/g	Uncorr. disp., %	Uncorr. cluster diam., nm	O_2 uptake per g_{cat}, µmol/g	% Red.	Corr. disp., %	Corr. cluster diam., nm
0.1 %Pt (ALD) 25 %Co (ALD) SiO_2	–	0.651	16.9	7.8	5.9	–	–	–	–	–	–	–
0.1 %Pt (ALD) 25 %Co (ALD) Al_2O_3 (ALD) on SiO_2	–	0.593	15.8	8.7	6.5	–	–	–	–	–	–	–
25 %Co (ALD) SiO_2	90.1	0.598	13.5	7.5	5.6	–	–	–	–	–	–	–
25 %Co (ALD) Al_2O_3 on SiO_2	79.7	0.578	14.1	8.9	6.7	50.2	2.4	43.6	524	18.5	12.8	8.1
0.1 %Pt (ALD) 25 %Co (IWI) Al_2O_3	92.1	0.230	5.0	14.6	11.0	134.7	6.3	16.3	1802	63.7	10.0	10.3
25 %Co (IWI) Al_2O_3	96.6	0.256	5.0	14.7	11.0	91.9	4.3	23.8	1354	47.9	9.2	11.2
0.1 %Pt (IWI) 25 %Co (IWI) Al_2O_3	101.5	0.286	5.5	11.6	8.7	141.8	6.7	15.4	1655	58.5	11.4	9.0
0.1 %Pt (IWI) 25 %Co (IWI) Al_2O_3 Trial #2	97.9	0.243	4.8	14.4	10.8	137.2	6.5	16.0	1644	58.2	11.1	9.3
20 %Co (IWI) PQ-SiO_2	263.9	0.842	5.9	13.5	10.1	25.5	1.5	68.5	1716	75.8	2.0	52.0
PQ-SiO_2	351.9	2.373	12.9	–	–	–	–	–	–	–	–	–
Catalox 150 γ-Al_2O_3	149.3	0.500	5.4	–	–	–	–	–	–	–	–	–

The catalyst activation conditions for chemisorption measurements were: 400 °C, 5 h, 33 %H_2 in helium, 30 cm^3/min flow rate

coordination (at low distance) and Co–Co (at higher distance) in the Co_3O_4 oxide. There is a clear signal decrease for the Co–O bond as the oxide converts to CoO and the peak for Co–Co coordination in the oxide moves to a shorter distance as CoO is formed, as expected. Finally, a peak for Co–Co in the metal is formed at even higher temperature.

There are two primary factors that influence the number of active sites, the surface Co^0 atoms, which are formed upon activation of a cobalt catalyst. The first factor was already discussed—the extent of cobalt reduction. However, the second factor is the average cobalt metal particle size. The second factor should not be understated. For standard catalysts prepared by aqueous impregnation of cobalt, despite a low extent of reduction of 30 % for 15 %Co/Al_2O_3 catalysts after a standard 350 °C reduction for 10 h in H_2, Jacobs et al. [11] observed that the number of active sites was 4 times higher than a corresponding 15 %Co/SiO_2 catalyst prepared by the same method and having over double the extent of reduction (64 %)—due to the fact that Al_2O_3 stabilized a much smaller particle size. This was the case despite the fact that SiO_2 exhibited a higher surface area. That is, the surface interaction with cobalt oxides was deemed to be the most important factor in controlling the particle size and extent of reduction of cobalt catalysts prepared by aqueous impregnation.

It should be noted, however, that procedures have been developed to produce smaller cobalt clusters on SiO_2-based catalysts. Direct reduction of Co/SiO_2 catalysts (in the form of cobalt nitrate) in H_2 has led to smaller cobalt cluster sizes relative to those prepared by standard air calcination followed by a H_2 reduction step for activation [33, 34]. Another method is the calcination of catalysts prepared with $Co(NO_3)_2$ precursor using a less oxidative gas relative to O_2, such as nitric oxide [35, 36]. In each of these cases, the reducibility of cobalt on silica decreased relative to standard calcined catalyst prepared by aqueous impregnation, due to the smaller cobalt size obtained and, thus, the greater interaction with the support.

In this case, the 25 %Co/SiO_2 catalyst was prepared by ALD. It is thus of interest to compare the average size of the catalyst to that of a standard catalyst prepared by impregnation. Fittings (Fig. 8) were carried out on EXAFS spectra recorded after high temperature reduction and cooling. Comparison of the calculated coordination numbers (Table 2) shows that the 25 %Co/SiO_2 ALD catalyst exhibits a larger particle size relative to the alumina supported catalysts. Moreover, in comparison with our earlier work using a 20 %Co/SiO_2 catalyst prepared by aqueous impregnation of cobalt, the coordination numbers are comparable (9.8 in this work versus 10.1 for the catalyst prepared by impregnation). However, the question must be raised as to whether it is fair to compare the catalysts after

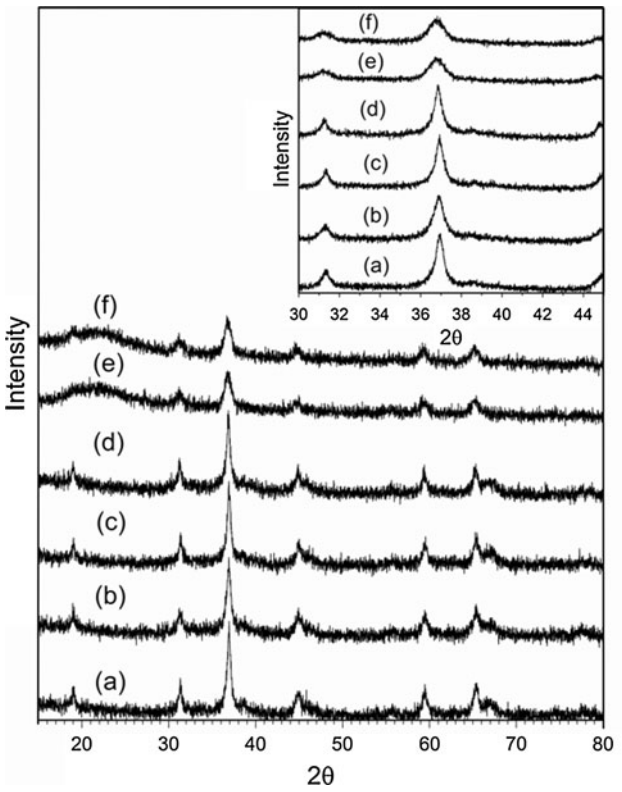

Fig. 1 X-ray diffraction profiles of Al_2O_3-supported catalysts, including (*a*) 25 %Co (IWI) Al_2O_3; (*b*) 0.1 %Pt (IWI) 25 %Co (IWI) Al_2O_3; (*c*) 0.1 %Pt (IWI) 25 %Co (IWI) Al_2O_3 (trial #2) (*d*) 0.1 %Pt(ALD) 25 %Co (IWI) Al_2O_3; (*e*) 25 %Co (ALD) 0.1 %Pt (ALD) Al_2O_3 on SiO_2; (*f*) 25 %Co (ALD) Al_2O_3 on SiO_2

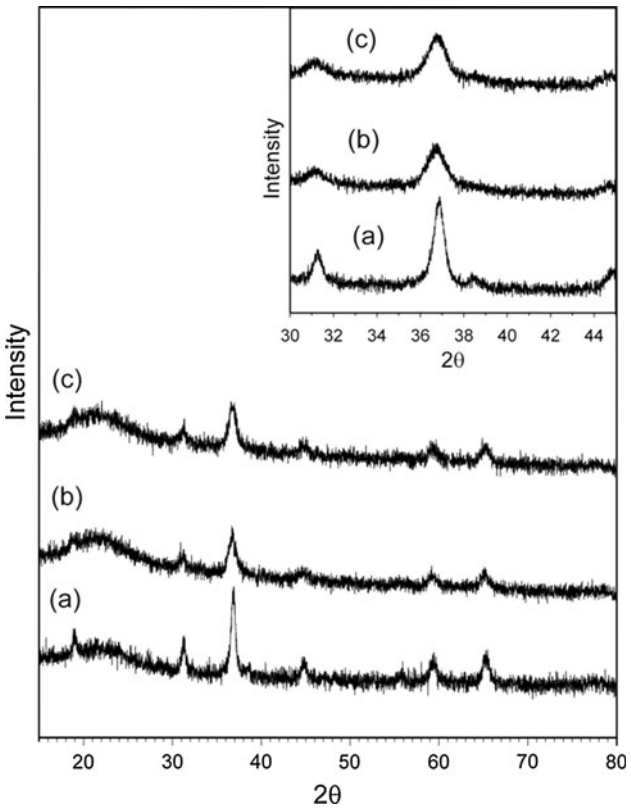

Fig. 2 X-ray diffraction profiles of SiO_2-supported catalysts, including (*a*) 20 %Co (IWI) PQ-SiO_2; (*b*) 0.1 %Pt (ALD) 25 %Co (ALD) SiO_2; and (*c*) 25 %Co (ALD) SiO_2

they have been subjected to treatment at such high temperatures, where sintering is likely.

The XRD results predict that smaller cobalt particles are generated by the ALD method, and one can further surmise, based on the earlier discussion, that a Co/SiO_2 catalyst prepared by ALD likely exhibits stronger surface interactions between the cobalt particles and the support—thereby hindering reduction—compared to a standard catalyst prepared by aqueous impregnation. Unfortunately, for the TPR-EXAFS/XANES run, there was not enough catalyst left over to run the unpromoted Co/SiO_2 ALD catalyst to demonstrate this unequivocally. Nevertheless, as will be shown in the next section, addition of Pt to Co/SiO_2 catalyst prepared by ALD significantly impacts CO conversion. It is well known that Pt addition increases the number of cobalt active sites by facilitating the reduction of cobalt oxides interacting with the support. Thus, the reaction testing results provide some evidence that, in the absence of a reduction promoter like Pt, the cobalt particles on Co/SiO_2 ALD catalysts are small enough (as demonstrated by XRD) such that significant surface interactions with the support exist that hinder their reduction.

In comparing the resulting cobalt particle size of Co/Al_2O_3 catalysts having 0.1 %Pt added by either ALD or IWI, the coordination number after high temperature reduction and cooling appears to be somewhat higher for the ALD catalyst relative to the IWI catalysts (8.9 versus 8.1 and 8.4, respectively), although the data are within experimental error of each other. If this is the case, one possibility is that the more facile reduction of cobalt oxides brought about by a greater interaction with Pt for the ALD catalyst resulted in greater agglomeration of cobalt metal. It should be noted that Soled et al. and Li et al. [33, 34] used the direct reduction of cobalt nitrates in order to slow the reduction process relative to the standard reduction of air calcined catalysts; the result was a considerably smaller cobalt particle size. In this case it would appear that the opposite case arose, where increasing the rate of reduction by using ALD Pt tended to increase the average cobalt particle size. A slightly larger cluster size and slightly lower site density were observed in hydrogen chemisorptions/pulse reoxidation results (Table 1). As will be demonstrated in the reactivity section to follow, despite the more facile reduction of cobalt with ALD Pt addition, the catalyst did not display a higher CO conversion rate relative to the Pt IWI catalyst, further confirmation of a slightly larger average cobalt particle size for the ALD Pt catalyst.

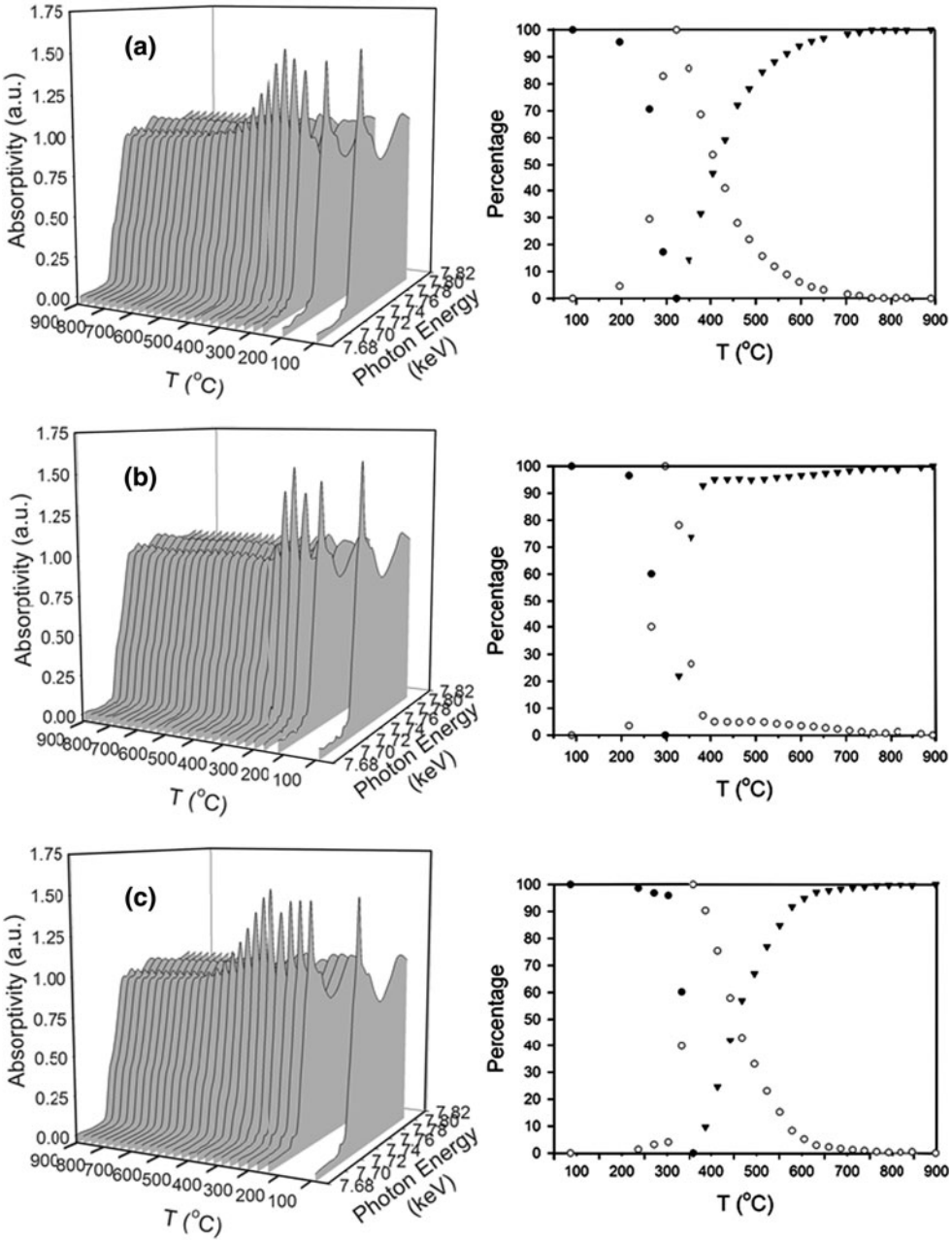

Fig. 3 (*left*) Normalized H_2-TPR-XANES spectra recorded near the Co K-edge and (*right*) linear combination fittings for (**a**) 0.1 wt% Pt/ALD on 25 wt% Co/ALD + on Al_2O_3 on SiO_2; (**b**) 0.1 wt% Pt/ALD on 25 wt% Co/ALD on SiO_2; and (**c**) 25 wt% Co on Al_2O_3 (CAER one step calcination). *Symbols* (*filled circles*) Co_3O_4; (*open circles*) CoO; (*filled triangles*) Co^0

3.4 Reference FT Experiments

Initial FT experiments were carried out using an empty reactor. There was a nominal level of CO conversion presumably due to the presence of a catalytic surface on the thermocouples and stainless steel tubes. To reduce the active catalytic surface effect of the reactor, the stainless tube and associated fittings were coated with a passivating alumina film using the ALD system. The level of CO conversion was reduced by about one-half when the stainless steel surfaces were coated with a 50 nm Al_2O_3 layer. Subsequent experimental runs were made with the ALD Al_2O_3-coated reactor.

3.5 Particulate Catalysts

3.5.1 Effect of Co Concentration on the FT Catalysts

A series of ALD cobalt-containing catalysts was made using silica support on which a 0.4 nm ALD Al_2O_3-coating had been deposited. These catalysts were first reduced in hydrogen at 350 °C, tested in a series of FT runs, reduced at 400 °C, and again tested in a series of FT runs. The results of the FT experiments are summarized in Fig. 9.

The level of CO conversion increased about linearly with the amount of ALD Co in the range of 9–25 % Co. Considering a catalyst pre-conditioned at 400 °C and a

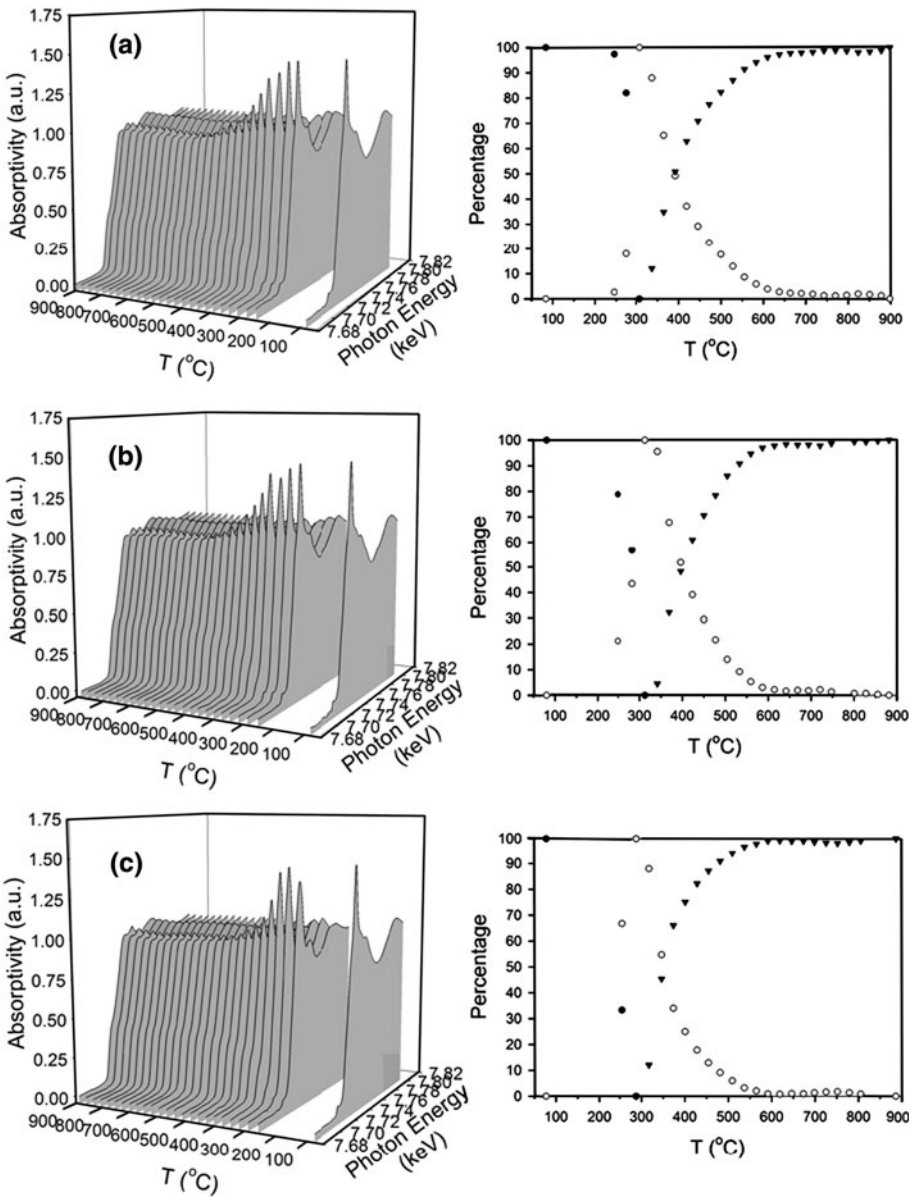

Fig. 4 (*left*) Normalized H_2-TPR-XANES spectra recorded near the Co K-edge and (*right*) linear combination fittings for (**a**) 0.1 wt% Pt on 25 wt% Co on Al_2O_3 (CAER prep by IWI); (**b**) 0.1 wt% Pt on 25 wt% Co on Al_2O_3 (CAER prep by IWI Trial #2); and (**c**) 0.1 % ALD/Pt on CAER 25 % Co on Al_2O_3. *Symbols* (*filled circles*) Co_3O_4; (*open circles*) CoO; (*filled triangles*) Co^0

reference reactor temperature of 280 °C, the level of CO conversion was estimated to be 4, 6, 12 and 16 % for Co loadings of 9, 11, 17, and 25 %, respectively. The selectivity of CO conversion to hydrocarbons when compared to total CO_2 conversion was in the range of 85–97 % for the latter three catalysts.

As shown in Fig. 9, the IWI catalyst exhibited a higher CO conversion than the ALD catalyst at a comparable Co loading. The selectivity of CO conversion to hydrocarbons was 96 % for the IWI catalyst and was similar to that of the ALD catalysts at 17–25 % loading. The lower activity for the ALD catalyst compared to the IWI catalyst may result from the ALD Al_2O_3 support layer, the ALD Cl, or both.

Figure 10 shows that catalysts consisting of 25 % Co prepared using the ALD technique on either silica or alumina ALD-deposited on silica had essentially the same CO conversion activity. This finding suggests that the support had little effect on the ALD Co catalysts. The 25 % IWI catalyst was about three times as active for CO conversion, and this difference was confirmed using a duplicate IWI catalyst with 25 % Co (Fig. 10). In summary, the IWI catalysts are more active for FT than the ALD catalysts at a comparable metal loading, and this difference appears to be due to a low extent of reduction (18.5 % for ALD relative to 47.9 % for IWI with 25 %Co Al_2O_3), as observed in hydrogen chemisorption/pulse reoxidation (Table 1). The result suggests that some ALD cobalt is suitably small enough to be interacting strongly with the support such that it does not undergo reduction even at 400 °C.

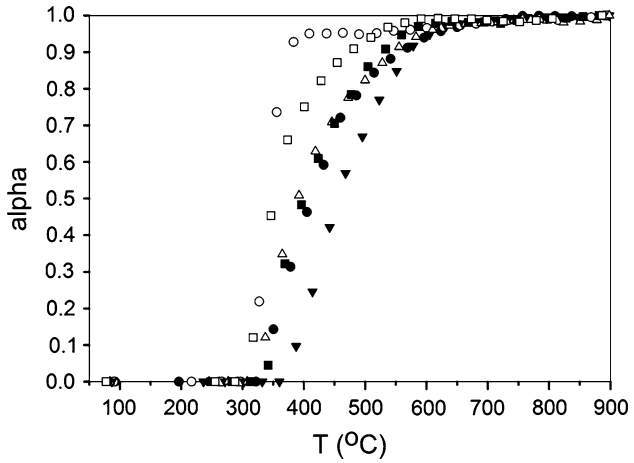

Fig. 5 Extent of CoO reduction to Co^0 (alpha) versus temperature for (*filled circles*) 0.1 wt% Pt/ALD on 25 wt% Co/ALD + on Al_2O_3 on SiO_2; (*open circles*) 0.1 wt% Pt/ALD on 25 wt% Co/ALD on SiO_2; (*filled triangles*) 25 wt% Co on Al_2O_3 (CAER one step calcination); (*open triangles*) 0.1 wt% Pt by CAER on 25 wt% Co on Al_2O_3; (*filled squares*) 0.1 % Pt on CAER 25 % Co; and (*open square*) 0.1 % ALD/Pt on CAER 25 % Co on Al_2O_3

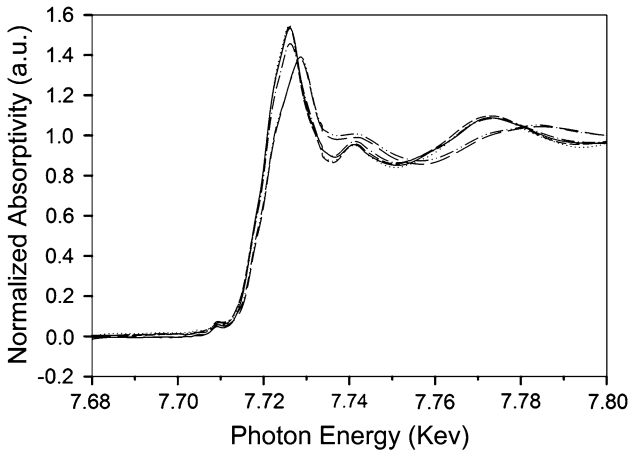

Fig. 6 Normalized XANES spectra for the point at which maximum CoO content was detected in the catalyst, including (*solid line*) 0.1 wt% Pt/ALD on 25 wt% Co/ALD + on Al_2O_3 on SiO_2 (~322.0 °C); (*dotted line*) 0.1 wt% Pt/ALD on 25 wt% Co/ALD on SiO_2 (~297.0 °C); (*dashed line*) 25 wt% Co on Al_2O_3 (CAER one step calcination) (~360.2 °C); (*dash-dot-dotted*) 0.1 wt% Pt by CAER on 25 wt% Co on Al_2O_3 (~307.6 °C); (*long dashed line*) 0.1 % Pt on CAER 25 % Co (~312.6 °C); and (*dash-dotted*) 0.1 % ALD/Pt on CAER 25 % Co on Al_2O_3 (~287.6 °C)

3.5.2 *Effect of Preconditioning Temperature Upon Catalyst Activity*

FT cobalt containing catalysts are preconditioned in H_2 to convert the surface oxide in the following steps: $Co_3O_4 \rightarrow$ CoO and CoO $\rightarrow Co^0$. The Co^0 is believed to be the active phase for the FT reaction. This route was indicated as previously reported [10] using TPR-XANES/EXAFS experimentation. The Co_3O_4 to CoO transformation occurred in a temperature range of about 150–400 °C. The CoO to Co^0 step depended strongly on the nature of the support with the reduction of CoO in strongly interacting Co/Al_2O_3 extending beyond 700 °C. Support type was found to be the key factor in determining the strength of the interaction and the rate at which the cobalt oxides underwent reduction. For both 15 and 25 % Co on Al_2O_3 the Co_3O_4 to CoO reduction reaction started at about 150 °C and appears to have been complete at about 400 °C and the reduction of CoO to Co^0 appears to have started at about 400 °C and continued to temperatures above 700 °C.

The temperature to be used for the Co catalyst preconditioning in the FT series was originally set at 350 °C, but it was subsequently increased to 400 °C, which was near the design limit of the unit. FT experiments were undertaken to confirm the effect of the preconditioning temperature upon catalyst activity.

The effect of preconditioning on FT cobalt catalyst activity is shown in Fig. 9. The FT activity of 9.4 % Co ALD coated catalyst when preconditioned at only 350 °C was only marginally better than that of an empty reactor. However, there was a 3–5 % increase of CO conversion when the catalyst was preconditioned at 400 °C. With a Co level of 17 %, there was about a 5 % increase of CO conversion when the catalyst preconditioning was increased from 350 to 400 °C. In the case of 15 % Co catalyst prepared by IWI, the increase of CO conversion level ranged from about 5 to 15 % in the 270° to 290° FT range when the preconditioning temperature was increased from 350 °C to 400 °C. Therefore, there is an obvious advantage in increasing the preconditioning temperature when testing Co-coated catalysts (without any promoters). Considering that the active surface of the FT catalyst is Co^0, further increasing the preconditioning temperature should be of advantage. However in our case, the operating temperature limits of the unit kept us from experimentation at higher temperatures.

3.5.3 *Effect of the Addition of Pt as a Promoter*

The addition of Pt as a promoter greatly enhanced the Co reduction process as noted in the TPRXANES/EXAFS study [10]. Therefore, a series of FT experiments was undertaken to observe the interaction of Pt addition and preconditioning temperature upon FT catalyst activity.

The results of experiments made with IWI catalysts are summarized in Fig. 11. The overall conversions of CO of these catalysts can be compared at a reactor temperature of 280 °C. The use of 15 % Co by IWI catalysts preconditioned at 350 and 400 °C resulted in CO conversions of 13 and 24 %, respectively. With the addition of 0.5 % Pt and a preconditioning temperature of 400 °C, the level of CO conversion increased to about 56 %. This confirms that the

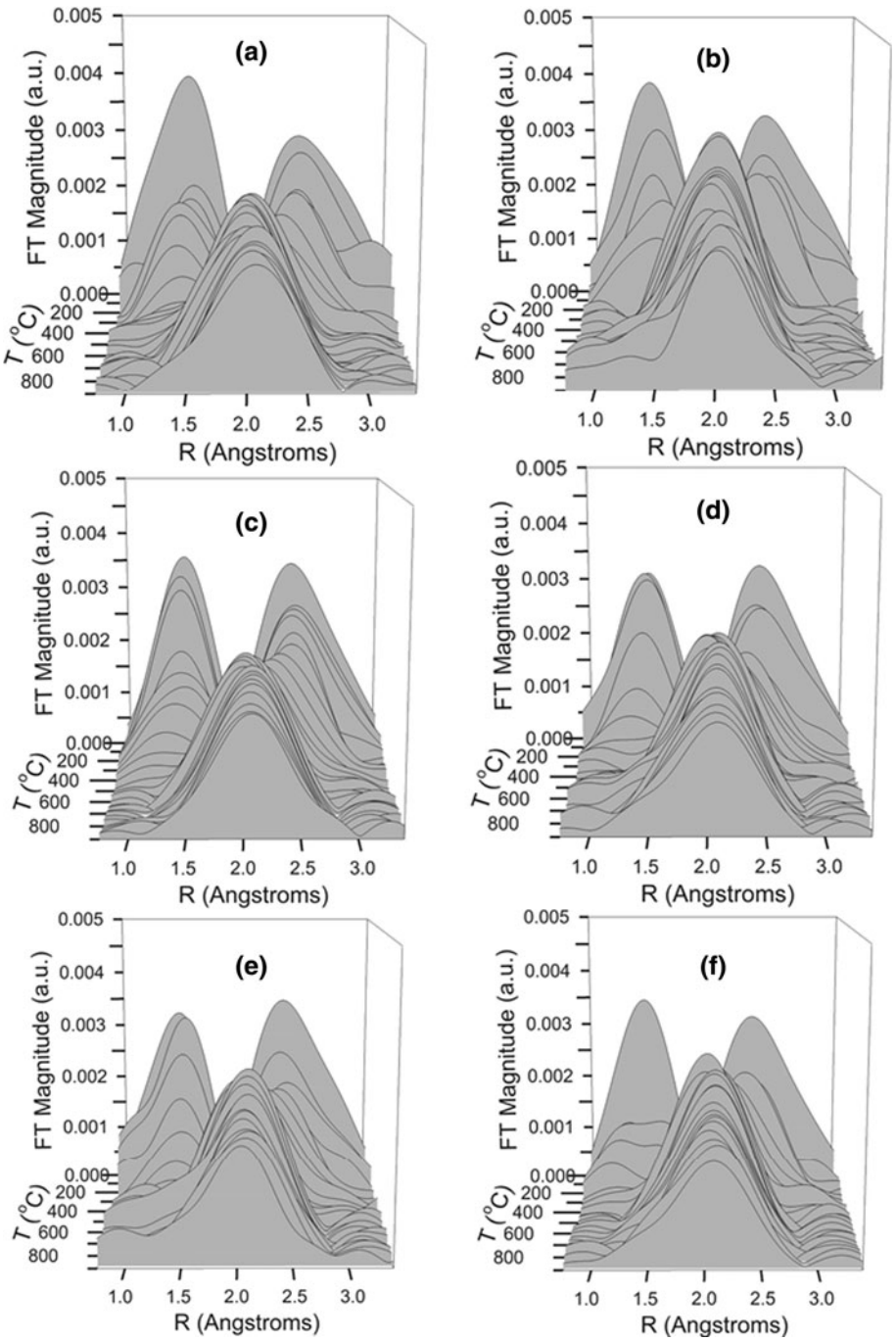

Fig. 7 EXAFS k^1-weighted Fourier transform magnitude spectra as a function of temperature, including (**a**) 0.1 wt% Pt/ALD on 25 wt% Co/ALD + on Al_2O_3 on SiO_2; (**b**) 0.1 wt% Pt/ALD on 25 wt% Co/ALD on SiO_2; and (**c**) 25 wt% Co on Al_2O_3 (CAER one step calcination); (**d**) 0.1 wt% Pt on 25 wt% Co on Al_2O_3 (CAER prep by IWI); (**e**) 0.1 wt% Pt on 25 wt% Co on Al_2O_3 (CAER prep by IWI Trial #2); and (**f**) 0.1 % ALD/Pt on CAER 25 % Co on Al_2O_3

addition of a promoter such as Pt greatly increases catalytic activity after preconditioning.

The results of FT experiments made with ALD-prepared catalysts with a support of Al_2O_3 deposited on SiO_2 are shown in Fig. 12. Again, the overall conversions of CO of these catalysts can be compared at a reactor temperature of 280 °C. The use of 17 % Co ALD catalysts preconditioned at 350 and 400 °C resulted in CO conversions of about 7 and 12 %, respectively. These levels of CO conversion were about one-half of those of the equivalent IWI catalysts.

As also noted in Fig. 12, the ALD deposition of Pt at a level of 0.5 % on a 25 % Co on ALD Al_2O_3 generated an active catalyst. Specifically, CO conversions were about 15 and 38 % for the 25 % Co catalysts without and with Pt, respectively (400 °C preconditioning).

Figure 13 provides a comparison between the ALD-Al_2O_3-deposited on SiO_2 and bare SiO_2 supported catalysts when the level of Co was 25 % and the preconditioning temperature was limited to 400 °C. The activities of the ALD Al_2O_3-deposited on SiO_2 and SiO_2 supported ALD

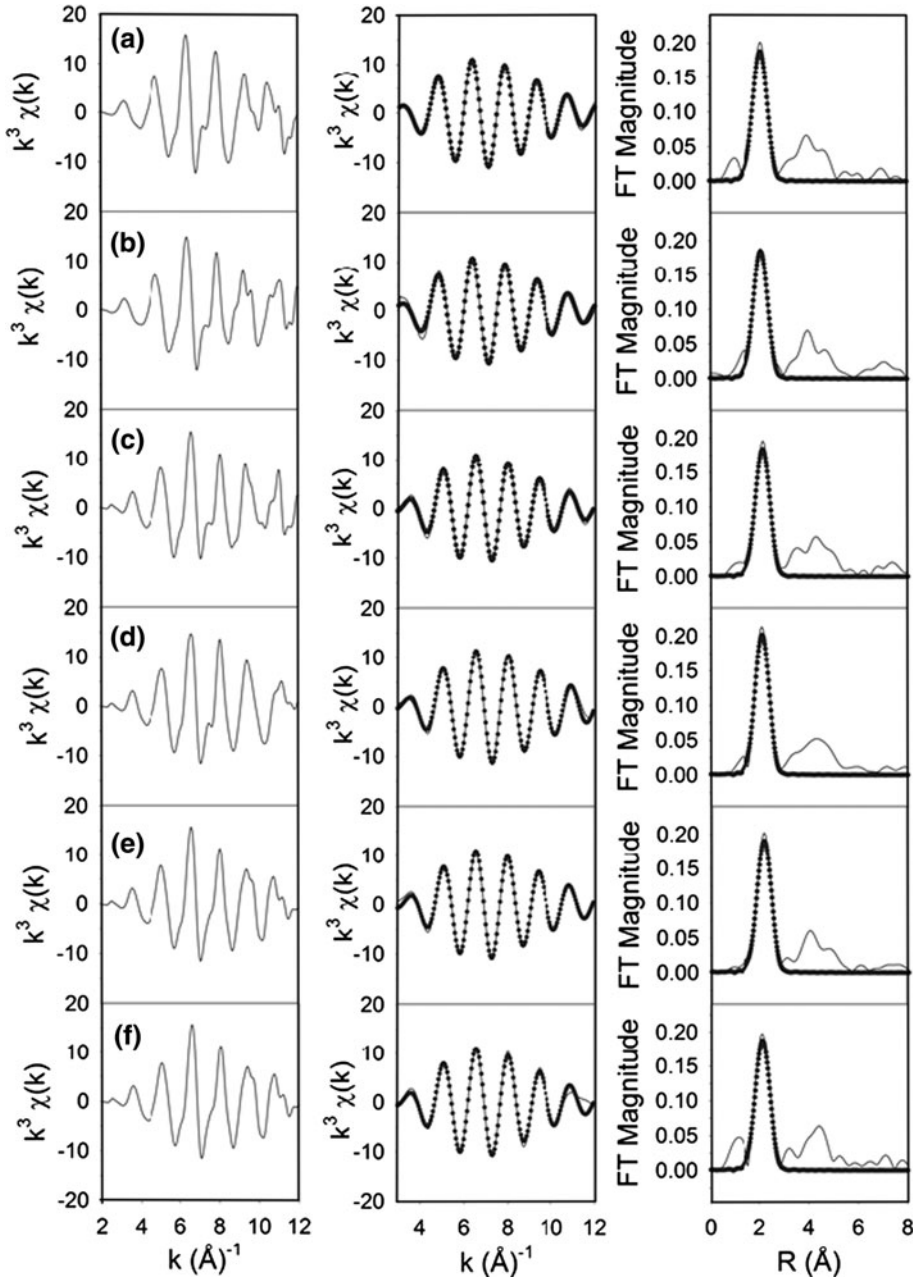

Fig. 8 Results of EXAFS fittings, including (*left*) raw $k^3 \cdot \chi(k)$ versus k data; (*middle*) filtered $k^3 \cdot \chi(k)$ versus k data and fitting; and (*right*) Fourier transform magnitude of data and first shell fitting of (**a**) 0.1 %Pt (ALD) 25 %Co (ALD) Al_2O_3 (ALD) on SiO_2, (**b**) 0.1 %Pt (ALD) 25 %Co (ALD) SiO_2, (**c**) 25 %Co (IWI) Al_2O_3, (**d**) 0.1 %Pt (IWI) 25 %Co (IWI) Al_2O_3, (**e**) 0.1 %Pt (IWI) 25 %Co (IWI) Al_2O_3 Trial #2, and (**f**) 0.1 %Pt (ALD) 25 %Co (IWI) Al_2O_3

Co catalysts with no promoter were equal. With the deposition of about 0.6 % and even 0.1 % Pt by ALD, the activity of the SiO_2 supported catalyst was about double that of the Al_2O_3 supported catalyst.

A comparison of experimental results of catalysts promoted with a low level of Pt, namely 0.1 %, is presented in Fig. 14. In all cases, the use of 0.1 % Pt as a promoter increased CO conversion activity. Table 1 confirms that the Pt addition increases the extent of reduction and thereby significantly improves the active sites density (e.g., 91.9 μmol H_2 desorbed/g for unpromoted versus 135–142 μmol H_2 desorbed/g for 0.1 %Pt promoted catalysts). The use of the ALD technique to deposit Pt increased the activity by about 15 %. However, the use of IWI to deposit this low level of Pt was shown to be more effective. The most active catalyst was prepared in which the Co-containing catalyst was first calcined and then impregnated with the Pt solution followed by a second calcination. An intermediate activity catalyst was also prepared in which the Pt solution was introduced prior to the Co calcination step. There remains some question of the difference of activities with order of calcination due to the results observed at about 265 °C. As noted previously from TPR-EXAFS/XANES results, ALD Pt was found to better facilitate reduction of cobalt oxides relative to IWI Pt, but the resulting average cobalt size appears to be higher. The

Table 2 Results of EXAFS fitting for data acquired near the Co K edge for catalysts reduced directly in the EXAFS multisample in dilute H_2

Catalyst	N Co–Co metal	R Co–Co metal (Å)	e_0 (eV)	σ^2 (Å^2)	*r*-factor
Co^0 foil	12 (set)	2.494	7.1	0.0070	0.0061
		(0.005)	(1.0)	(0.0002)	
0.1 %Pt (ALD) 25 %Co (ALD) Al_2O_3 (ALD) on SiO_2	9.9	2.492	−4.7	0.0109	0.0068
	(0.9)	(0.006)	(1.0)	(0.0007)	
0.1 %Pt (ALD) 25 %Co (ALD) SiO_2	9.8	2.487	−5.2	0.0111	0.0142
	(1.5)	(0.010)	(1.8)	(0.0013)	
25 %Co (IWI) Al_2O_3	8.9	2.481	4.7	0.0110	0.0056
	(0.8)	(0.006)	(1.0)	(0.0007)	
0.1 %Pt (IWI) 25 %Co (IWI) Al_2O_3	8.0	2.467	2.8	0.0094	0.013
	(1.0)	(0.008)	(1.5)	(0.0010)	
0.1 %Pt (IWI) 25 %Co (IWI) Al_2O_3	8.4	2.495	6.5	0.0102	0.002
Trial #2	(0.5)	(0.004)	(0.6)	(0.00045)	
0.1 %Pt (ALD) 25 %Co (IWI) Al_2O_3	8.9	2.482	5.0	0.0109	0.018
	(1.34)	(0.010)	(1.7)	(0.0013)	

The fitting ranges for the Co–Co metal first shell fitting were approximately $\Delta k = 3.0–12.0$ Å^{-1} and $\Delta R = 1.5–2.8$ Å

Note that S_0^2 was fixed at 0.90 as a first approximation

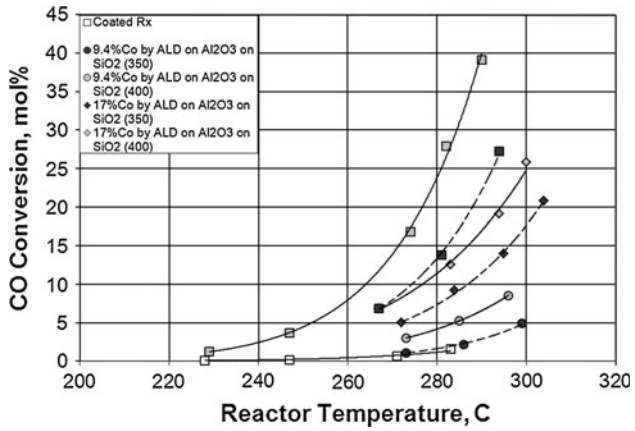

Fig. 9 CO conversion vs. reaction temperature with ALD and IWI Co on Al_2O_3 support catalysts with 350 and 400 °C reduction temperature

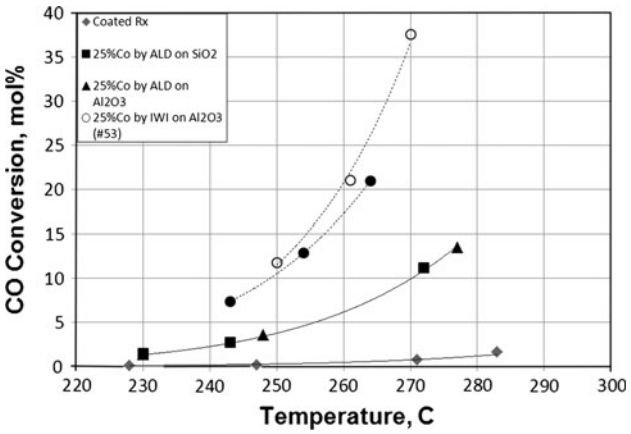

Fig. 10 CO conversion vs. reaction temperature with various supports with 25 % ALD and IWI Co catalysts and 400 °C reduction

latter point could explain the lower activity of the ALD Pt catalyst despite its slightly faster reduction rate.

The effectiveness of depositing low levels of Ir and Ru on the 25 % Co catalyst is shown in Fig. 15. The Ir results and evaluations have been previously reported [37]. Ir deposited by both incipient wetness and ALD was shown to be a more effective promoter than Pt or Ru. Again the incipient wetness technique was best. Ru was shown to be only about 60 % as effective as Ir.

The FT runs exhibited similar linear Arrhenius correlations with comparable slopes. The overall average activation energy of the various ALD-prepared Co catalysts was 28.6 kcal/mol. The average of all of the FT runs with Co-containing FT catalysts, including those with low levels of Pt promoter, was about 29.2 kcal/mol.

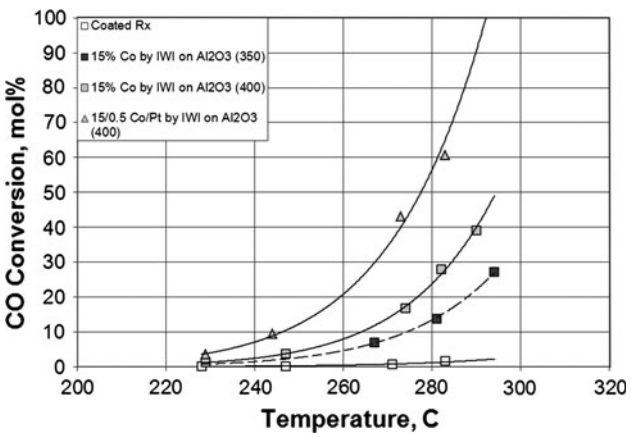

Fig. 11 CO conversion vs. reaction temperature; effect of Pt addition upon IWI Co activity with 350 and 400 °C reduction

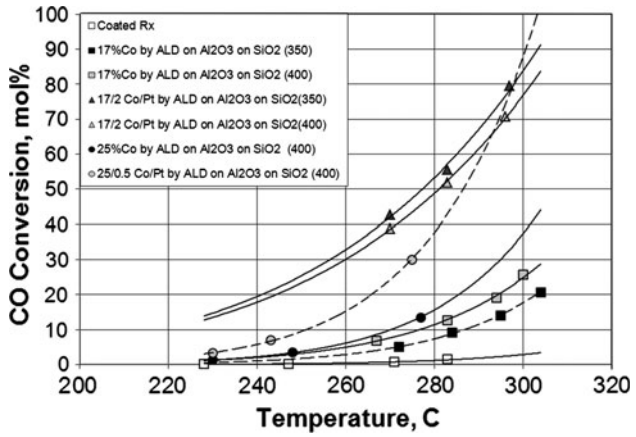

Fig. 12 Effect of Pt addition upon ALD Co activity with 350 and 400 °C reduction

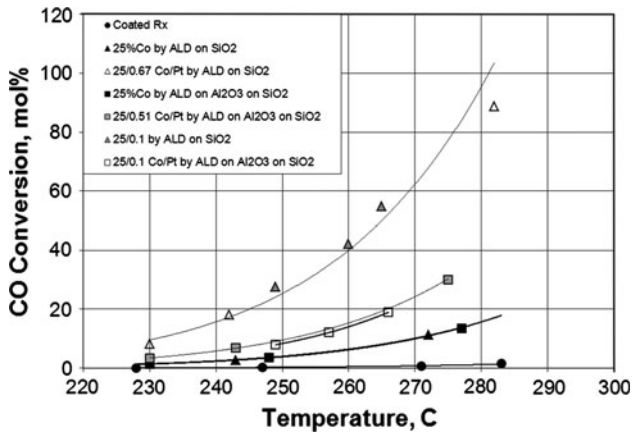

Fig. 13 CO conversion vs. reaction temperature; comparison of support and Pt addition with 25 % Co ALD catalysts and 400 °C reduction

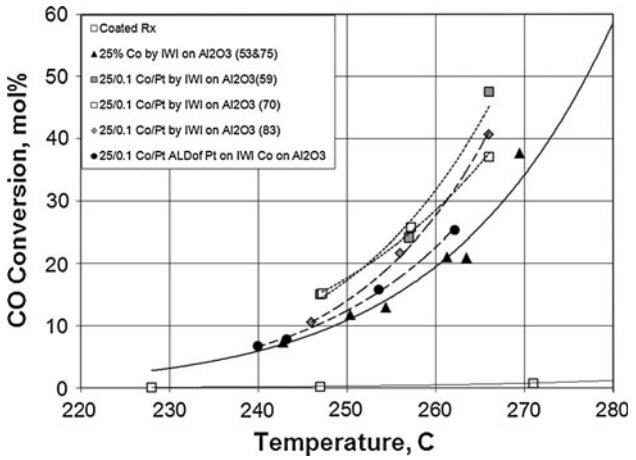

Fig. 14 CO conversion vs. reaction temperature; comparison of Pt addition techniques with 25 % Co catalysts with 400 °C reduction

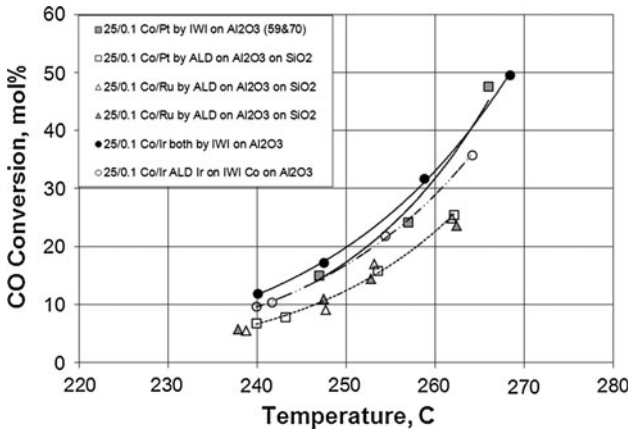

Fig. 15 CO conversion vs. reaction temperature; comparison of various promoters with 0.1 % deposited on 25 % IWI Co catalysts with 400 °C reduction

Considering the above discussion of catalyst properties, SEM scans were made of selected catalyst samples. A comparison of the surfaces of the 25 % Co by IWI on alumina and 25 % Co by ALD on ALD-alumina on silica catalysts is shown in Fig. 16. The first catalyst has a smoother surface than the second. This is consistent with the above reported catalyst properties.

4 Conclusions

Active catalysts for the Fischer–Tropsch (FT) reduction of carbon monoxide formed by both incipient wetness impregnation (IWI) and atomic layer deposition (ALD) have been prepared and demonstrated using a continuous-flow catalytic-bed unit. A catalyst consisting of IWI Co deposited on an Al_2O_3 support was more active than ALD-deposited Co on a silica support. This in turn was more active than an ALD-prepared Co surface deposited on an ALD-coated Al_2O_3 surface deposited on silica.

The addition of Co promoters including Pt, Ir and Ru with either ALD or IWI deposition has been shown to strongly affect the catalyst pre-conditioning step. CO conversion results were consistent with previously reported TPR-XANES/EXAFS experiments observing the nature of chemical transformations occurring during the activation of cobalt-based FT catalysts in hydrogen. Specifically, there exists a 2-step reduction process involving Co_3O_4 to CoO and CoO to Co^0 transformations. The extent of catalyst preconditioning was strongly affected by the reduction temperature (with 400 °C preferred) and the level of promoter deposition.

The addition of Pt greatly promoted the preconditioning of Co-containing catalysts. This observation was valid for both ALD and IWI prepared catalysts. The most effective ALD-prepared FT catalyst was one containing cobalt

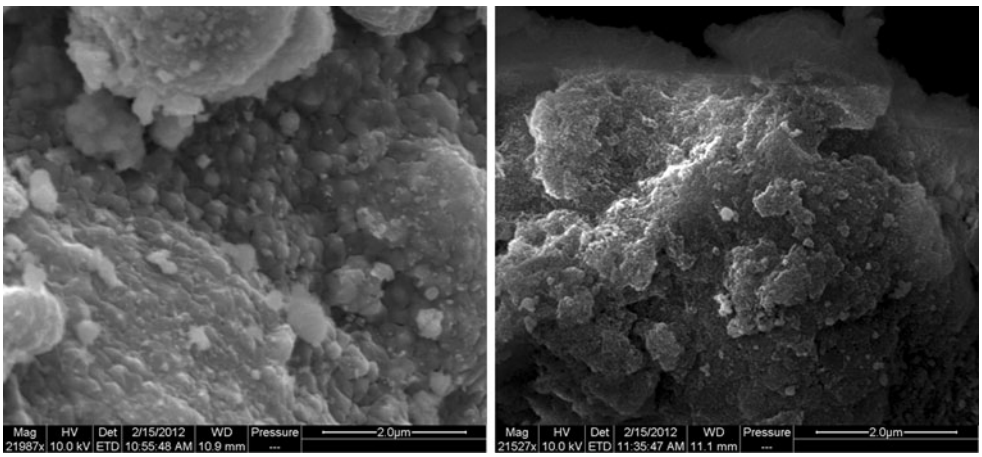

Fig. 16 SEM scans at about 26,000 magnification of 25 % Co by IWI on alumina (*left*) and 25 % Co by ALD on alumina by ALD on silica (*right*)

deposited on a silica support that was subsequently ALD coated with about 0.6 % Pt promoter. As noted previously, it appears that smaller Co particles in close interaction with the support were likely formed by the ALD method compared to standard impregnation catalysts, and to the point that reduction of cobalt oxides was hindered. Pt addition apparently facilitated their reduction, leading to a greater number of active sites and boosting the CO conversion rate. This catalyst had about the same FT activity as a similar Co and Pt on Al_2O_3 catalyst prepared by IWI. The FT activity of ALD-coated Co catalysts on Al_2O_3 was about linear with Co level from about 9–25 %. Therefore, there is a question about the uniformity of the ALD deposition process and atomic level interactions with the Al_2O_3 deposited surface. For reference, catalysts containing only Pt and Ru that were ALD-deposited on an ALD-Al_2O_3 coated catalyst supports were found to be relatively inactive.

The preconditioning of Co-containing catalysts was tested at temperatures of 350 and 400 °C. The higher temperature was much more effective, as was also indicated in previously reported TPR-XANES/EXAFS experiments.

The average activation energy of the rate of CO conversion was about 29.2 kcal/mol when all of the Co-containing catalysts other than those with high Pt promoter levels were taken into account.

Acknowledgments The work carried out at the CAER was supported in part by funding from a grant from NASA (#NNX07AB93A), as well as the Commonwealth of Kentucky. Argonne's research was supported in part by the U.S. Department of Energy (DOE), Office of Fossil Energy, National Energy Technology Laboratory (NETL) under Project AA-10-15; 49261-00-107. The use of the Advanced Photon Source was supported by the U.S. Department of Energy, Office of Science, Office of Basic Energy Sciences, under Contract DE-AC02-06CH11357. MRCAT operations are supported by the Department of Energy and the MRCAT member institutions. J.W. Elam was supported as part of the Institute for Atom-efficient Chemical Transformations (IACT), an Energy Frontier Research Center funded by the U.S. Department of Energy (DOE), Office of Science, Office of Basic Energy Science. The SEM scans were prepared by D.J. Schroeder and A. Hubaud using a FEI Quanta 400F ESEM unit. The electron microscopy was accomplished at the Electron Microscopy Center for Materials Research at Argonne National Laboratory, a U.S. Department of Energy Office of Science Laboratory operated under Contract No. DE-AC02-06CH11357 by UChicago Argonne, LLC.

References

1. Schulz H, Claeys M (1999) Appl Catal A Gen 186:1
2. Steynberg A, Dry M (eds) (2004) Stud Surf Sci Catal 152
3. van der Laan GP, Beenackers AACM (1999) Catal Rev Sci Eng 41:255
4. Satterfield CN (1996) Heterogeneous catalysis in industrial practice, 2nd edn. Krieger Publ. Co., Malabar
5. Davis BH, Technology Development for Iron Fischer–Tropsch Catalysts, Final Technical Report, Dec. 18, 1990–Dec. 17, 1993, DE96005561, DOE/PC/90056–T17, 12/31/96
6. Iglesia E (1997) Appl Catal A Gen 161:59
7. van Steen E, Claeys M, Dry ME, van de Loosdrecht J, Viljoen EL, Visagie JL (2005) J Phys Chem B 109:3575
8. Bezemer GL, Bitter JH, Kuipers HPCE, Oosterbeek H, Holewijn JE, Xu XD et al (2006) J Am Chem Soc 128:3956
9. Borg Ø, Dietzel PDC, Spjelkavik A, Tvetenc EZ, Walmsleyd JC, Diplasb S (2008) J Catal 259:164
10. Jacobs G, Ji Y, Davis BH, Cronauer DC, Kropf AJ, Marshall CL (2007) Appl Catal A Gen 333:177
11. Jacobs G, Das TK, Zhang Y, Li J, Racoillet G, Davis BH (2002) Appl Catal A Gen 233:263
12. Guczi L, Bazin D, Kovacs I, Borko L, Schay Z, Lynch J, Parent P, Lafon C, Stefler G, Koppany Z, Sajo I (2002) Top Catal 20:129
13. Kogelbauer A, Goodwin JG Jr, Oukaci R (1996) J Catal 160:125
14. Schanke D, Vada S, Blekkan EA, Hilmen AM, Hoff A, Holmen A (1995) J Catal 156:85
15. Hilman AM, Schanke D, Holmen A (1996) Catal Lett 38:143
16. Hilmen AM, Schanke D, Hanssen KF, Holmen A (1999) Appl Catal A Gen 186:169

17. Jacobs G, Chaney JA, Patterson PM, Das TK, Maillot JC, Davis BH (2004) J Synchrotron Radiat 11:414
18. Jacobs G, Chaney JA, Patterson PM, Das TK, Davis BH (2004) Appl Catal A Gen 264:203
19. Ma W, Jacobs G, Ji Y, Bhatelia T, Bukur DB, Khalid S, Davis BH (2011) Top Catal 54:757
20. Bazin D, Borko L, Koppany Zs, Kovacs I, Stefler G, Sajo L, Schay Z, Guczi L (2002) Catal Lett 84:169
21. George SM (2010) Chem Rev 110:111
22. Feng YH, Elam JW, Libera JA, Pellin MJ, Stair PC (2010) J Catal 269:421
23. Elam JW, Groner MD, George SM (2002) Rev Sci Inst 73:2981
24. Christensen ST, Elam JW (2010) Chem Mater 22:2517
25. Ott AW, Klaus JW, Johnson JM, George SM (1997) Thin Solid Films 292:135
26. Nilsen O, Lie M, Foss S, Fjellvag H, Kjekshus A (2004) Appl Surf Sci 227:40
27. Aaltonen T, Alen P, Ritala M, Leskela M (2003) Chem Vapor Deposition 9:45
28. Jacoby M (2001) Chem Eng News 79:33
29. Ressler T (1998) J Synchrotron Radiat 5:118
30. Ravel B (2001) J Synchrotron Radiat 8:314
31. Rehr JJ, Zabinsky SI, Albers RC (1992) Phys Rev Lett 69:3397
32. Newville M, Ravel B, Haskel D, Stern EA, Yacoby Y (2005) Phys B 208/209:154
33. Soled SL, Iglesia E, Fiato RA, Baumgartner JE, Vroman H, Miseo S (2003) Top Catal 26:101
34. Li J, Jacobs G, Das TK, Zhang YQ, Davis BH (2002) Appl Catal 236:67
35. Sietsma JRA, Meeldijk JD, den Breejen JP, Versluijs-Helder M, van Dillen AJ, de Jongh PE, de Jong KP (2007) Angew Chem Int Ed 46:4547
36. Jacobs G, Ma W, Davis BH, Cronauer DC, Kropf AJ, Marshall CL (2010) Catal Lett 140:106
37. Cronauer DC, Jacobs G, Linganiso L, Kropf AJ, Elam JW, Christensen ST, Marshall CL, Davis BH (2011) Catal Lett 141:968